Desalination and Water Treatment
www.deswater.com

doi: 10.5004/dwt.2017.21097

84 (2017) 279–291
July

Preparation, characterization and Pd(II) adsorption characteristics of chitosan–AC composites from electroless plating solutions

Yennam Rajesh[a], Nagireddi Srinu[a], Gummalla Namrata[b], Uppaluri Ramgopal[a,*]

[a]*Department of Chemical Engineering, Indian Institute of Technology Guwahati, Guwahati 781039, Assam, India, Tel. +91 361 2582260; emails: ramgopalu@iitg.ernet.in (U. Ramgopal), rajeshiitg09@gmail.com (Y. Rajesh), nagireddi@iitg.ernet.in (N. Srinu)*
[b]*Department of Chemical Engineering and Technology, Birla Institute of Technology, Mesra, Jharkhand 835215, India, email: namrata.gummalla@gmail.com*

Received 18 January 2017; Accepted 1 July 2017

ABSTRACT

This study targets the comparative efficacy of impregnated and cross-linked chitosan–activated carbon composite adsorbents for Pd(II) adsorption from Ethylenediaminetetraacetic acid (EDTA)-containing electroless plating (ELP) solutions. Specific novelty of the addressed research in the article corresponds to adsorption and desorption characteristics of said adsorbents for Pd(II) recovery from synthetic ELP solutions that can be characterized to have complex solution chemistry than aqueous solutions. The Brunauer–Emmett–Teller analyses indicated maximum surface area of cross-linked adsorbent (1,317 $m^2 \cdot g^{-1}$). The adsorbent provided a highest capacity (8.08–70.14 $mg \cdot g^{-1}$) and removal percentage (84.17%–97.04%) for variant Pd(II) solution concentration. For ELP solutions, the monolayer Pd(II) adsorption capacities are maximum (90.91/95.6 $mg \cdot g^{-1}$) for cross-linked chitosan AC adsorbent. These findings infer that Pd(II)-adsorbed chitosan cross-linked activated carbon can be developed as waste to value product for low temperature catalysis applications.

Keywords: Pd(II) adsorption; Electroless plating solution; EDTA; Chitosan; Activated carbon

1. Introduction

Platinum group metals (PGMs) and particularly palladium have several functional applications in industries. With excellent physical and chemical properties such as corrosion resistance, electrical conductivity, catalytic activity and high melting point, Pd(II) has several applications in the manufacture of conductors, telephone circuits, heat and corrosion resistant parts, dental and medical devices, tools and materials in medical industries and noble metal-supported catalysts for petrochemical and automobile industries [1].

Continuous demand for palladium-based products infers on a greater demand for the noble metal. Palladium ores are rare and their low concentration in the earth's crust is responsible for its high cost. To meet the demands, it is imperative to consider the recovery and recycle of Pd(II) from secondary sources such as metal finishing industries, rinse waters and post-consumer scrapes. Recently, spent automobile catalysts have emerged as major secondary sources for both palladium and platinum. However, only 20% metal has been reported to be recycled from such sources [1,2].

Conventional methods for palladium and PGMs recovery are solid phase extraction, solvent extraction, coprecipitation [3], membrane separation [4], leaching [5], cloud point extraction [6], sorption and post-sorption [7]. Among these, sorption processes are often regarded to be promising due to their ability to recover noble metals from dilute acid solutions. Compared with other conventional methods, adsorption has several other promising features such as environmentally friendly, lower cost, availability, profitability, ease of operation and high removal efficiency [8].

In the past decade, researchers studied adsorbents such as activated carbon, clays, metal oxides, silica and zeolite

* Corresponding author.

for the removal and recovery of heavy and precious metals. Activated charcoal/carbon (AC) has been extensively studied due to its high adsorption capacity, adsorption rate, porous structure, large internal surface area and good abrasion resistance. In such investigations, AC demonstrated its ability to adsorb wide varieties of undesirable species from gaseous and liquid phase systems. On the other hand, the removal and recovery of Pd(II) from aqueous and synthetic wastewater solutions was studied using various synthetic chelating ion-exchange resins [9,10].

An alternative to synthetic chelating resins is adsorption using biopolymers. Since recent times, biopolymer-impregnated and cross-linked AC-based adsorbents have been studied for several applications. Among biopolymers, chitosan is preferred due to its wider availability and lower cost in comparison with synthetic chelating polymers [11,12].

During metal adsorption, the hydroxyl and amine functional groups of chitosan enable stronger binding with metal ions through chelation. In addition, electrostatic interactions could occur and thereby facilitate ion exchange or formation of ion pair. These interactions are dependent on metal type, chemical constituents of interacting medium and pH of solution. Till date, chitosan and its derivatives, such as cross-linked chitosan with synthetic polymeric structures, chitosan beads, impregnated chitosan activated carbon composites, cross-linked chitosan–AC adsorbents, and so on, have been studied for the removal of heavy and precious metals [13–17]. In several such investigations, aqueous solutions with simpler chemical constitution were deployed to target adsorbent separation characteristics. However, it is well known that real wastewaters from metal finishing industries have complex solution chemistry and hence, carried out studies may not be effective to infer on the competence of these adsorbents for noble metal recovery and reuse [18,19].

From materials engineering perspective, two important studies targeted the preparation of chitosan–AC adsorbents by impregnation [20] and cross-linking [12]. Among these, the cross-linked chitosan–AC adsorbent has been evaluated to possess higher Brunauer–Emmett–Teller (BET) surface area and sorption capacity. Thereby, in comparison with the AC, the cross-linked adsorbent has been evaluated to capture higher quantity of CO_2 from biohydrogen, biogas and flue gas mixtures. For cross-linked chitosan–AC adsorbent, Pd(II) adsorption studies were conducted within the initial Pd(II) concentration range of 40–300 mg·L^{-1} and for aqueous solutions. The obtained results may or may not be relevant for the recovery of Pd(II) from industrial wastewater streams.

This study emphasizes on the relevance of chitosan-based AC adsorbent for Pd(II) recovery and reuse from synthetic electroless plating (ELP) solution with compositions similar to real ELP solutions. Considering various avenues for further research, this work addresses preparation and characterization of cross-linked and impregnated chitosan–AC adsorbents. Subsequent characterizations of adsorbents were carried out using BET, Fourier transform infrared spectroscopy (FTIR) and scanning electron microscope (SEM) instruments. Eventually, batch adsorption studies were conducted to evaluate equilibrium Pd(II) adsorption characteristics with synthetic ELP solutions with and without *N*-cetyl-*N*,*N*,*N*-trimethyl ammonium bromide (CTAB) surfactant. Desorption studies were carried out to illustrate the potential of adsorbents for the adsorbed Pd(II) recovery. Fitness studies were conducted to evaluate the relevance of standard adsorption models for the measured equilibrium data. The following section elaborates on experimental procedures that were adopted for adsorbent preparation and subsequent studies.

2. Materials and methods

Palladium chloride (99.9%, SRL Chemicals Pvt. Ltd., India), Na_2EDTA (Merck, India), liquor ammonia (25%, Merck, India), CTAB (Merck, India) and millipore water (Milli-Q) were used to prepare Pd(II)-containing synthetic ELP solutions. Solution pH was adjusted by using analytical grade HCl, NaOH solutions and pH meter (VSI-301).

2.1. Preparation of Pd(II) stock solution

$PdCl_2$ stock solution (1,000 mg·L^{-1}) was prepared using synthetic ELP bath composition presented in Table 1 [21,22]. The synthetic solution was prepared by mixing precise amounts of various precursors in deionized water for 15 min at 120 rpm using orbital shaker. Solutions with variant Pd(II) concentrations were prepared by diluting stock solution. All chemicals/reagents used were of analytical grade purity. The ELP solution composition essentially refers to a stabilizer (Na_2EDTA) and an optional cationic surfactant (CTAB) in an alkaline media prepared with liquor ammonia. For all adsorption studies, the Pd(II) solution concentration varied between 50 and 500 mg·L^{-1}.

2.2. Preparation of activated charcoal–chitosan composites

2.2.1. Chitosan-impregnated activated charcoal adsorbents

The procedure involved in the preparation of chitosan-impregnated activated charcoal adsorbent has been outlined elsewhere [20] and has been followed to obtain chitosan-impregnated AC adsorbent without using CTAB surfactant. To prepare chitosan-impregnated AC adsorbents, first, activated charcoal powder was washed with deionized water to remove fines and dirt. Then, it was dried in an oven at 100°C for 24 h before impregnation process was conducted. Later, AC was sieved to sizes ranging from 60 to 65 μm to prepare two types of adsorbents, namely, chitosan-impregnated activated charcoal (CH-AC-I) and chitosan-surfactant-impregnated

Table 1
Composition of synthetic Pd(II) electroless plating solutions

Name of the component	Palladium solution concentration (mg·L^{-1})					
	50	100	200	300	400	500
$PdCl_2$ (mg·L^{-1})	83.31	166.63	333.27	499.90	666.54	833.17
Na_2EDTA (g·L^{-1})	1.39					
NH_3 solution (25%), mL·L^{-1}	10.33					
CTAB, mg·L^{-1} (if any)	335–1,340					

activated charcoal (CH-AC-IS). CH-AC-I was prepared with wetness impregnation method with a solution concentration of 2 g·L^{-1} of AC and variant initial concentrations of chitosan (0.1–2 g·L^{-1}). Using similar solution concentrations, CH-AC-IS adsorbent was prepared using additional CTAB surfactant (1–2 critical micelle concentration [CMC] solution concentration). The impregnated adsorbents were prepared by subjecting the mixture of AC, chitosan and surfactant of the adsorbent, chitosan and surfactant (if any) in an orbital shaker (agitation speed of 200 rpm at 25°C) for 3 d. After this step, the modified AC powder was separated from chitosan solution by adopting filtration process. The final chitosan concentration in solution was evaluated by measuring the absorbance of filtrate using a UV–visible spectrometer (Lamda 35, PerkinElmer, China) at a wavelength of 197 nm (obtained after conducting calibration studies). Finally, CH-AC-I and CH-AC-IS were dried in a hot air oven at 100°C for 24 h. The quantity of chitosan impregnation on the activated charcoal was further verified by evaluating the weight gain of the adsorbent after impregnation process. Using the measured data, chitosan adsorption capacities on the adsorbent and removal percentage (from the solution) during impregnation process have been determined using expressions presented in section 2.3.

2.2.2. Cross-linked chitosan–activated charcoal adsorbent

The method adopted for the preparation of cross-linked chitosan–activated charcoal (CH-AC-C) adsorbent has been outlined elsewhere [11,12] and is briefly presented as follows. To prepare oxalic acid–treated adsorbent, 20 g of AC was added to 0.2 M oxalic acid and the mixture was stirred for 4 h. Thereby, the AC was filtered and washed with deionized water and dried in an oven at 70°C for 12 h. Eventually, chitosan–oxalic acid gel was achieved by continuously agitating 10 g of chitosan in 1 L of 0.2 M oxalic acid at 45°C–50°C for 1 h. To the gel, 20 g of acid-treated AC was added slowly and stirred for 16 h at 45°C–50°C. Subsequently, the gel–AC mixture was added dropwise to 1 L of NaOH (0.7 M) precipitation bath at 50°C. Finally, the cross-linked adsorbent was filtered from NaOH bath and washed several times with deionized water to achieve neutral pH. Prior to usage in characterization and batch adsorption studies, the CH-AC-C adsorbent was dried in a hot air oven at 50°C for 6 h.

2.3. Batch adsorption characteristics

Batch experiments were performed using 0.05–0.3 g of CH-AC-C powder and 50 mL of ELP solution. In these experiments, the initial Pd(II) concentration was varied from 50 to 500 mg·L^{-1} at a pH of 9–10. All batch adsorption experiments were performed with 50 mL containing 250 mL flasks at specified Pd(II) concentrations at 25°C in a wrist action shaker (Labtop; LSI-125/R; India) operated for 1–5 h at 200 rpm. After this step, the mixture was filtered using Whatman filter paper (No. 40) to obtain filtrate for Pd(II) concentration analysis using atomic absorption spectrophotometer (AAS; Varian spectra, FS240, India, equipped with air–acetylene flame detector) operated at a wavelength of 247.6 nm [23]. Using the measured concentrations, capacity and removal percentage of Pd(II) have been determined using the following expressions:

$$\text{Removal, (\%)} = \frac{\left(C_o - C_e\right)}{C_e} \times 100 \quad (1)$$

$$\text{Adsorption capacity, (mg/g)} = \frac{\left(C_o - C_e\right)}{W} \times V \quad (2)$$

where C_o is the initial concentration of Pd(II) in ELP solution in mg·L^{-1}, C_e is the equilibrium adsorption concentration of chitosan in mg·L^{-1}, V is the volume of solution in mL and W is the weight of the adsorbent dosage in g.

2.4. Adsorbent characterization

FTIR spectral analysis was conducted using FTIR instrument (PerkinElmer, PE-RXI, range: 500–4,000 cm^{-1}) for the determination of various functional groups in CH-AC-C adsorbent. SEM (Leo, 1430 VP, Carl Zeiss, Germany) was deployed to determine surface morphology and elemental composition of CH-AC-I, CH-AC-IS and CH-AC-C adsorbents. BET surface areas and monolayer volumes were measured using a surface area analyzer (Beckman Coulter, SA-3100) to generate a nitrogen adsorption isotherm at 150°C. In this study, before measurement, the samples were degassed using helium at 200°C for 2 h. Laser particle size analyzer (M/s Malvern Instruments Ltd., UK) was used to estimate the average particle size distribution of CH-AC-I, CH-AC-IS and CH-AC-C adsorbents. Point of zero charge (PZC) was determined for CH-AC-C using procedures summarized in our earlier work [21,24]. Conceptually, it is well known that the adsorbent exhibits maximum adsorption at an adsorbent pH value that is just greater than the PZC [25].

2.5. Desorption studies

For CH-AC-C adsorbent, Pd(II) batch desorption studies were conducted using adsorbent obtained after batch adsorption studies, with an initial solution concentration of 300 mg·L^{-1}. This adsorbent was evaluated to have a capacity of 44.34 mg·g^{-1} for chosen Pd(II) concentration. Batch desorption studies were conducted with 0.1 M HCl and 0.1 M NaOH solutions prepared with millipore water. For batch desorption experiments, 0.12 g of adsorbent was used to achieve saturated desorption in 50 mL of reagent volume. Desorption experiments were conducted for a time period of 300 min. Subsequently, using final solution concentrations evaluated from AAS analysis, mass balance was conducted to estimate Pd(II) surface concentration on adsorbent after desorption. Eventually, Pd(II) recovery after desorption was evaluated using initial and final Pd(II) adsorbent concentrations.

2.6. Fitness of equilibrium and kinetic models

The fitness of measured equilibrium adsorption data was evaluated for Langmuir and Freundlich isotherms. Assuming complete monolayer coverage on homogenous adsorbent surface without any interaction between adsorbed ions, Langmuir equilibrium isotherm model is expressed as [26]:

$$\frac{C_e}{q_e} = \frac{1}{bq_{\max}} + \frac{1}{q_{\max}} C_e \quad (3)$$

where C_e represents equilibrium adsorption concentration of Pd(II) (mg·L^{-1}), q_e represents mass of solute adsorbed per mass of adsorbent at equilibrium (mg·g^{-1}) and q_{max}, b and C_o represent Langmuir monolayer capacity (mg·g^{-1}), Langmuir equilibrium constant and initial concentration of Pd(II) in aqueous solution (mg·L^{-1}).

Based on the Langmuir isotherm model parameters, the favourability towards adsorption is expressed in terms of the separation factor (K_R) as follows:

$$K_R = \frac{1}{(1 + bC_o)} \tag{4}$$

where K_R evaluated within the range of 0–1 indicates favourable adsorption.

Assuming exponential distribution of active centres with characteristics of heterogeneous surface and infinite surface coverage, Freundlich isotherm model is expressed as [27]:

$$\log\ q_e = \log\ k_f + m\ \log\ C_e \tag{5}$$

where k_f and m are the Freundlich isotherm constants.

Pseudo-first-order and pseudo-second-order models have been tested for their fitness to represent the kinetics of Pd(II) adsorption on CH-AC-C adsorbent [28]. The pseudo-first-order model to represent adsorption kinetics is expressed in terms of Lagergren equation [29]:

$$\log(q_e - q_t) = \log(q_e) - \frac{k_1}{2.303}t \tag{6}$$

where q_e, q_t, t and k_1 represent mass of solute adsorbed per mass of adsorbent at equilibrium (mg·g^{-1}), mass of solute adsorbed per mass of adsorbent at time t (mg·g^{-1}), agitation time (min) and first-order rate constant (min^{-1}), respectively.

On integration, the above expression is expressed as [30]:

$$\frac{t}{q_t} = \frac{1}{k_2 q_e^2} + \frac{1}{q_e}t \tag{7}$$

where q_e is the mass of solute adsorbed per mass of adsorbent at equilibrium (mg·g^{-1}), t is the agitation time (minutes), k_2 is the pseudo-second-order rate constant (g·mg^{-1}·min^{-1}).

For both equilibrium and kinetic models, errors associated with fitness of experimental data for the models were evaluated using following expressions:

$$Er_i = \frac{\left|C_i^{\exp} - C_i^{\text{model}}\right|}{C_i^{\exp}} \times 100 \tag{8}$$

$$\text{Ermax} = \text{Max}\left(\text{Er}_i\right) \tag{9}$$

$$\text{Ermin} = \text{Min}\left(\text{Er}_i\right) \tag{10}$$

$$\text{Eravg} = \frac{\sum_{i=1}^{n}\text{Er}_i}{n} \tag{11}$$

$$\text{RMSE} = \frac{\sqrt{\sum_{i=1}^{n}\text{Er}_i^2}}{n} \tag{12}$$

where Er, i, n, Er_{max}, Er_{min}, $\text{Er}_{average}$, Er_{rms} are error function, index for batch adsorption experiment corresponding to specific initial Pd(II) solution concentration, total number of batch adsorption experiments carried out with varying concentration, maximum error, minimum error, average error and root mean square (RMS) error, respectively.

3. Results and discussion

3.1. Chitosan adsorption characteristics for impregnated adsorbents

Based on calibration chart prepared for variant chitosan aqueous solution concentration of 0.1–1 g·L^{-1}, the chitosan removal percentage and capacity of CH-AC-I adsorbent varied from 59.73% to 17.05% and 14.93 to 0.42 mg·g^{-1}, respectively. However, for the CH-AC-IS adsorbent and for 1 CMC CTAB solution concentration, corresponding variations in chitosan removal percentage and capacity are 37.42% and 9.32 mg·g^{-1}, respectively. For comparison, literature data are not available and hence, it is intended that these experimental findings would serve as a reference for preparation of chitosan-impregnated AC adsorbents.

3.2. Adsorbent characterization

3.2.1. Surface area and pore size analysis

Activated charcoal was modified with chitosan using direct impregnation, surfactant-assisted impregnation and cross-linking to develop chitosan–AC composite adsorbents. Table 2 summarizes physical properties of chitosan-modified AC adsorbents. It can be analyzed that the BET surface area for CH-AC-C was obtained as 13,177 m^2·g^{-1}, which is higher than the values obtained for CH-AC-I and CH-AC-IS. Thus, impregnation did not enhance BET surface area and is an ineffective technique to achieve good quality chitosan–AC composite adsorbents. Among adsorbents, it can be observed from Table 2 that CH-AC-C adsorbent possessed a total pore volume, Langmuir surface area of 1.1117 mL·g^{-1} and 1,256.93 m^2·g^{-1}, respectively. It is anticipated that adsorbent with highest BET surface area will

Table 2
BET characterization parameters of AC, CH-AC-I, CH-AC-IS and CH-AC-C adsorbents

S.No.	Physical properties	AC	CH-AC-I	CH-AC-IS	CH-AC-C
1	BET surface area (m^2·g^{-1})	1,057	787	914	1,317
2	Total pore volume (mL·g^{-1})	0.6567	0.5227	0.7200	1.1117
3	Langmuir surface area (m^2·g^{-1})	1,197.5	833.83	1,125.331	1,256.23

exhibit highest adsorption efficiency and facilitate lowest adsorbent dosage.

Fig. 1(a) presents N_2 adsorption–desorption isotherms of CH-AC-C adsorbent. It can be observed that the isotherms were Type IV and the existence of H_4 hysteresis loop confirms existence of narrow slit-like pores [31]. In addition, it can be seen that the isotherm rises sharply during early stages of adsorption. This accounts for micropore filling effect and N_2 adsorption later on did not indicate significant enhancement in adsorption.

Fig. 1(b) represents Barrett–Joyner–Halenda (BJH) pore size distribution [32] of CH-AC-C that was obtained for both adsorption and desorption. Pore size distribution indicates that adsorbent possessed cylindrical pores and BJH analysis provided sharper peaks than isotherm data presented in Fig. 1(a). Fig. 1(c) illustrates variation in obtained pore area distribution with pore diameter. The figure confirmed that the adsorbent pore area was more sensitive to adsorption process than desorption. This is in agreement with the trends presented in relevant literature [12].

3.2.2. SEM characterization

SEM images of raw AC, prepared (CH-AC-I and CH-AC-C) and Pd(II)-adsorbed (Pd-E-CH-AC-C) adsorbents are illustrated in Figs. 2(a)–(d). It can be observed from Fig. 2(a) that raw activated charcoal had regular plain sponge-like surface. Figs. 2(b) and (c) indicate progressive changes and well-developed pores on AC surface for chitosan-impregnated AC and cross-linked AC adsorbents. The pore formation of CH-AC-I and CH-AC-C is due to chitosan bonding with the adsorbent surface. Due to this, enabled structural changes occurred and contributed to alterations in porous structure. In addition, Fig. 2(d) conveys structural variation in the adsorbent that was brought forward by Pd(II) adsorption on active sites of CH-AC-C adsorbent.

3.2.3. FTIR analysis

FTIR analysis was conducted for raw AC, CH-AC-I, CH-AC-C adsorbents and Pd(II)-adsorbed CH-AC-C adsorbents. Additional nomenclature in the article refers to Pd-E-CH-AC-C for Pd(II)-adsorbed cross-linked chitosan–AC adsorbent that was obtained after adsorption with ELP solution and Pd-E(S)-CH-AC-C refers for Pd(II)-adsorbed cross-linked chitosan–AC adsorbent obtained after adsorption with CTAB-containing ELP solution. The FTIR spectra for all adsorbents are presented in Fig. 3. FTIR analysis indicated existence of several functional groups on adsorbent surface. For the raw sample (AC), several peaks exist at wave numbers of 3,526, 3,300, 2,416, 2,328, 1,721, 1,520, 1,330 and 970 cm^{-1}. For CH-AC-I sample (chitosan-impregnated AC) peaks exist at wave numbers of 3,514, 3,309, 2,412, 2,301, 1,764, 1,521, 1,336 and 960 cm^{-1}. For CH-AC-C (cross-linked chitosan–AC), peaks can be observed at wave numbers of 3,512, 3,309, 2,420, 2,303, 1,732, 1,525, 1,350 and 966 cm^{-1}. For Pd-E-CH-AC-C and Pd-E(S)-CH-AC-C adsorbent samples (obtained after Pd(II) adsorption with ELP solutions), peaks exist at 3,520, 3,290, 2,418, 2,295, 1,759, 1,529, 1,328 and 956 cm^{-1}. Thus, several spectral peaks can be observed to have shifted from low to high intensity. Spectral–functional group interactions indicate OH stretching (3,500 cm^{-1}), C–H aliphatic stretching (2,920 cm^{-1}), –O–CH_3 of alkoxy group (2,858 cm^{-1}), C–H aldehydes (2,720 cm^{-1}), C=O aromatic stretching (2,350 cm^{-1}), stretching of C–O or O–H deformation in carboxylic acids (1,747 cm^{-1}), C–O stretching of aromatic ethers, esters and phenols (1,280–1,240 cm^{-1}), C–C stretching (700 cm^{-1}). It is well known that oxygen of OH

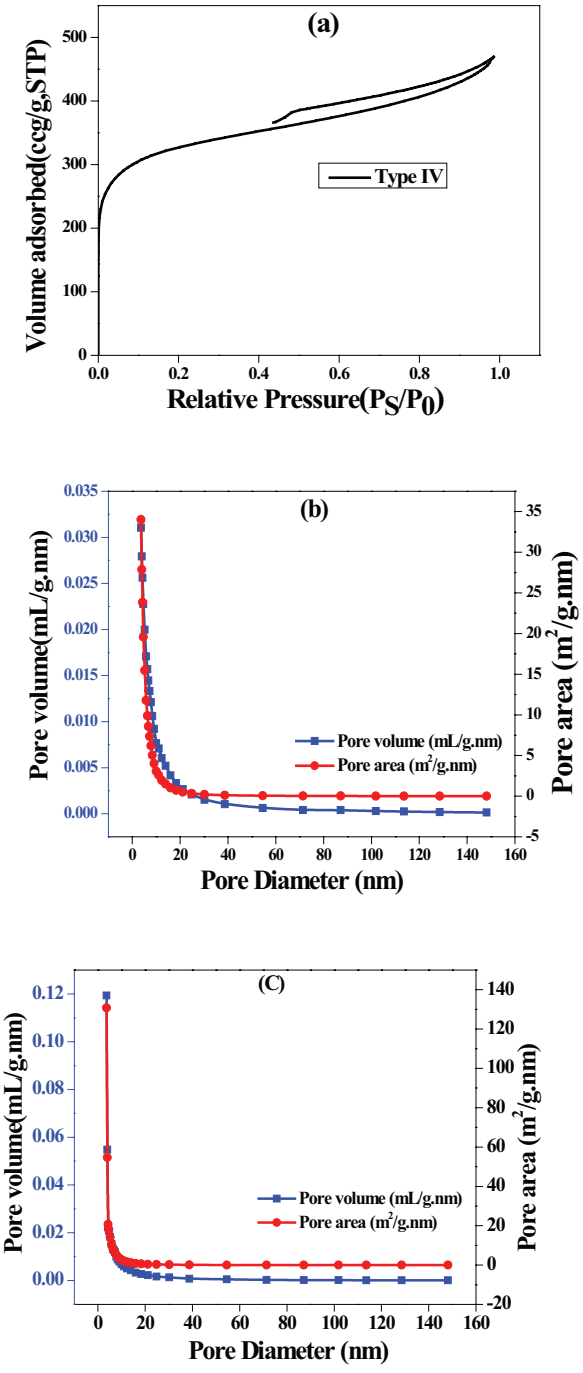

Fig. 1. BET surface area plots for CH-AC-C adsorbent: (a) BET isotherm (Type IV); (b) adsorption BJH pore volume and pore area distribution and (c) desorption BJH pore volume and pore area distribution.

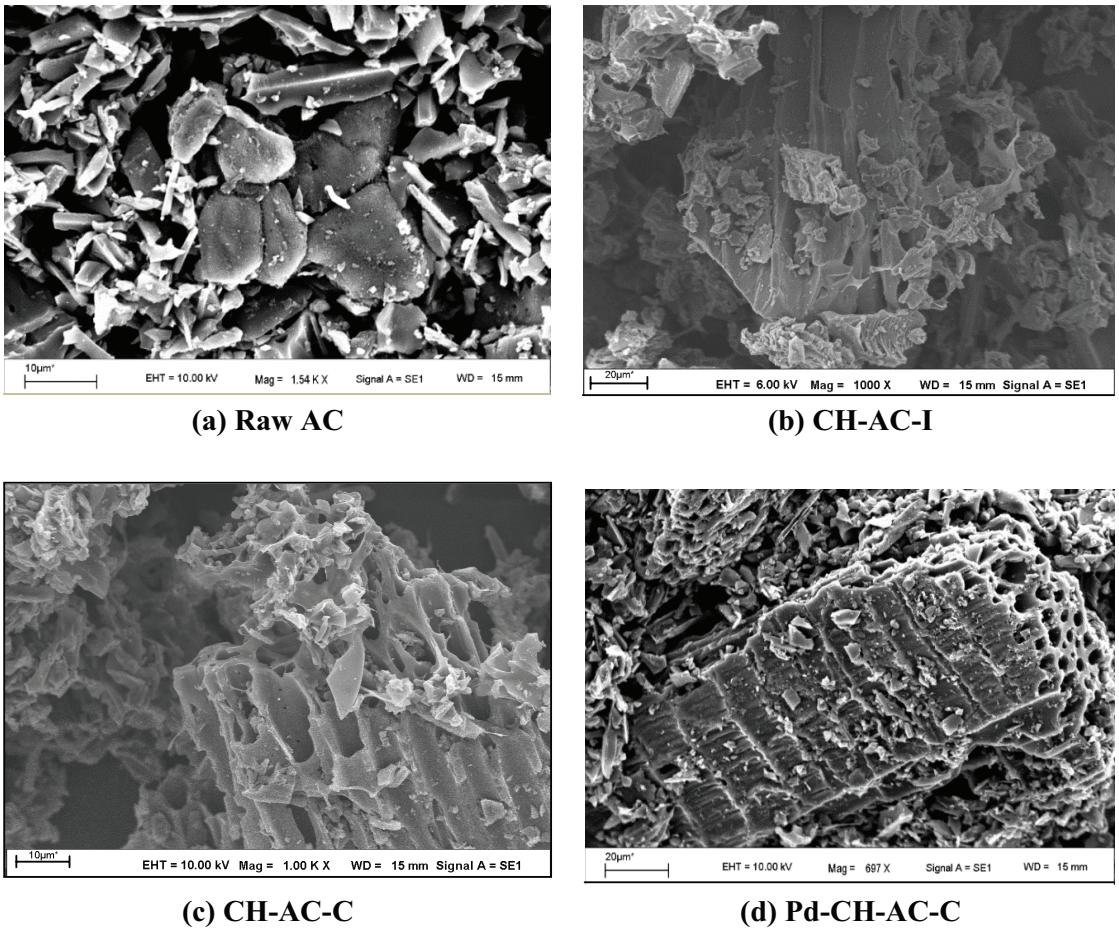

Fig. 2. SEM micrographs for various adsorbent samples. (a) Raw AC, (b) CH-AC-I, (c) CH-AC-C and (d) Pd-E-CH-AC-C.

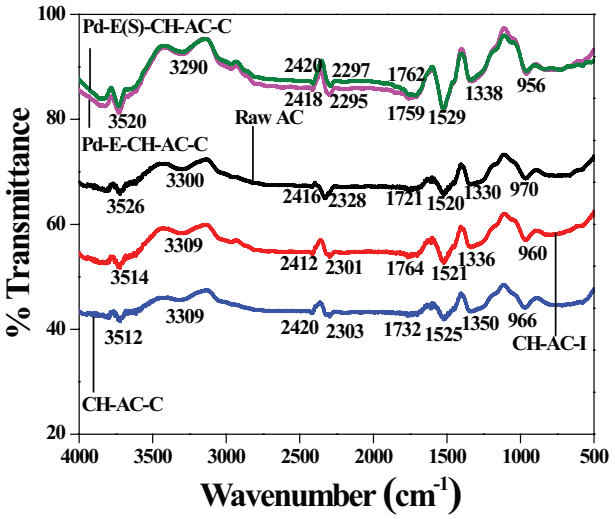

Fig. 3. FTIR spectra of raw AC, CH-AC-I, CH-AC-C, Pd-E-CH-AC-C and Pd-ES-CH-AC-C adsorbents.

bond has two lone pair of electrons that enables bonding of positively charged metal ions. Similarly, O–CH_3, C=O, CHO, COOH, C=O have lone pair of electrons on which Pd(II) undergoes chemisorption [12]. Therefore, FTIR spectral analysis conveys that strong possibilities exist for irreversible chemisorption and these have to be quantitatively analyzed from adsorption and desorption studies.

Based on the SEM characterization and FTIR analysis, a graphical representation of the impregnated and cross-linked chitosan–AC composite adsorbents is presented in Fig. 4. The graphical representation in the figure is based on the following reasoning and analysis. The FTIR analysis indicates no variations in the peaks correspond to various functional groups for all samples (AC, impregnated AC and cross-linked AC samples). Hence, it is affirmed that chemical changes did not occur to the samples on cross-linking or impregnation. In general, AC has micropores and mesopores and on impregnation, the organic moieties might have blocked the pores to significantly reduce the surface area and pore volume. This is confirmed by the BET surface analysis of impregnated samples. However, after cross-linking activity, it can be observed that the BET surface area enhanced with no additional functional groups evaluation after FTIR analysis. Hence, it is presumed that cross-linking facilitated structural alterations due to oxalic acid-based treatment and thereby promoted enhanced adsorption of chitosan to the microporous and mesoporous structure. It is further to be noted that while impregnated is a mere physical activity, cross-linking

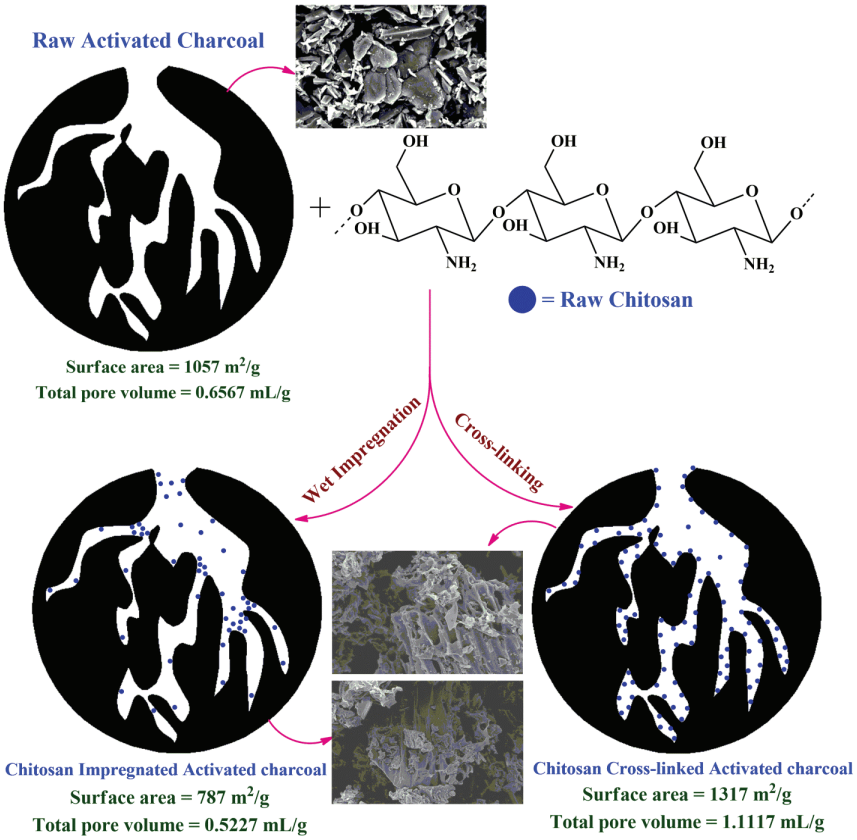

Fig. 4. Pictorial representation of cross-linked and impregnated chitosan–AC composite adsorbents.

involved digestive process. Therefore, it is hypothesized that the adopted cross-linking procedure facilitated structural alterations in the AC porous morphology and thereby provided higher surface area of the cross-linked AC adsorbent. Hence, the adopted procedure is regarded to be excellent due to the fact that cross-linking allowed both effective adsorption of chitosan to the AC microporous structure as well as enhancement in the structural morphology of the AC adsorbent. The available literature data do not elaborate on the presented hypothesis but is indicative to the very fact that cross-linked AC with chitosan using procedure followed in this work provided higher CO_2 capture from biohydrogen, biogas and flue gas mixtures [20]. The cross-linked chitosan has been reported to have higher surface area than AC in the said literature. Hence, these observations in the literature are affirming to the above presented hypothesis.

3.3. Batch adsorption

To analyze adsorption performance of CH-AC-C, optimality of adsorption parameters, such as pH, contact time and adsorbent dosage, was evaluated based on hierarchical selection procedure. For these experimental investigations, synthetic ELP solution without CTAB surfactant was used. Optimum solution pH was assessed by considering fixed choice of adsorbent dosage (2 g·L^{-1}), contact time of 360 min and an initial Pd(II) solution concentration of 50 mg·L^{-1}. At optimum pH of 12, second set of batch adsorption experiments were conducted with varying time intervals and fixed value of adsorbent dosage (2 g·L^{-1}). The initial Pd(II) solution concentration was 50 mg·L^{-1}. After identifying optimal contact time as 300 min and pH as 12, third set of batch adsorption experiments were conducted for optimum contact time, pH (obtained from first and second sets of adsorption experiments), 50 mg·L^{-1} Pd(II) solution concentration and with variant adsorbent dosage from 1 to 7 g·L^{-1}.

3.3.1. Effect of pH

Fig. 5(a) presents the effect of pH on the Pd(II) adsorption characteristics using CH-AC-C adsorbent. For variation in pH and contact time from 2 to 14 and 50 to 300 min, respectively, the Pd(II) removal percentage and adsorption capacities of CH-AC-C varied from 35.96% to 81.16% and 8.99 to 20.29 mg·g^{-1}, respectively. The figure also confirms that the maximum removal percentage of 87.36% at a metal uptake of 21.84 mg·g^{-1} can be obtained at 12 pH, which is the optimal pH for the adsorbent. In this regard, it is important to note that the literature conveys that for Biopolymer modified carbon (BPMC) adsorbent and aqueous Pd(II) solutions, for the batch adsorption parameters of 2 pH, 300 min contact time and 10 g·L^{-1} adsorbent dosage, the Pd(II) removal percentage and capacity are 98% and 16.98 mg·g^{-1} respectively [12]. Thus, it can be seen that characteristics of Pd(II) adsorption on CH-AC-C for synthetic ELP solutions were significantly lower than those obtained for aqueous solutions. Solution pH affects metal ion solubility, concentrations of counter ions on functional groups of adsorbent and degree of ionization of the

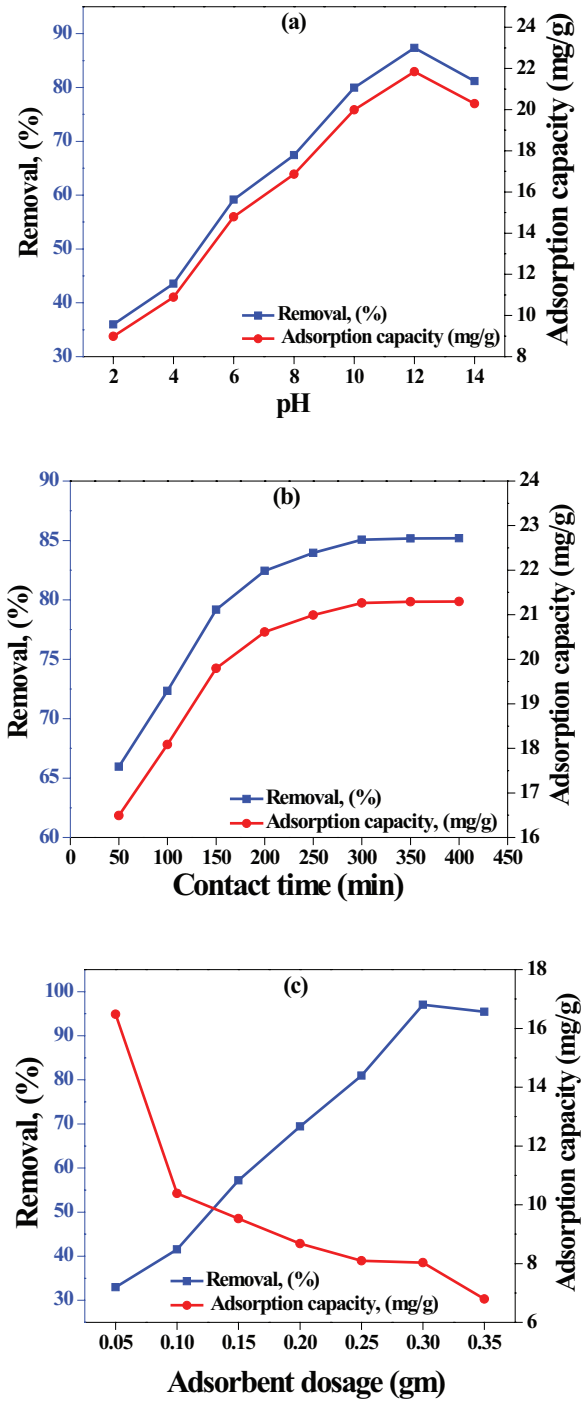

Fig. 5. Effect of variation in (a) pH, (b) contact time and (c) adsorbent dosage on adsorption capacity and removal efficiency using CH-AC-C adsorbent.

adsorbate. As shown, metal removal enhanced with increasing pH from 2 to 12 and eventually declined at higher pH. This is due to the fact that at low pH, H^+ enables protonation effect and this does not favour adsorption of Pd(II) on AC [25,33]. As pH increases, protonation effect reduces and availability of OH^- on adsorbent surface favours electrostatic attraction of Pd(II) ions. Beyond pH 12, there might be complexification of EDTA and NH_3 with Pd(II) and this is not favourable for the adsorption of Pd(II) onto CH-AC-C. Observed pH for maximum adsorption was at 12. The obtained optimal pH for CH-AC-C adsorbent is in good agreement with the optimal pH of 10.5 reported in the literature for Pd(II) adsorption from leached cyanide solutions on AC adsorbent [34].

3.3.2. Effect of contact time

Fig. 5(b) shows variation of metal uptake and removal efficiency with contact time. As indicated, for a pH of 12 and adsorbent dosage of 2 $g{\cdot}L^{-1}$, a variation in contact time from 50 to 400 min facilitates a variation in removal percentage and capacity from 65.9% to 85.20% and 16.49 to 21.29 $mg{\cdot}g^{-1}$, respectively. From Fig. 5(b), it can be observed that optimal contact time is 300 min at which maximum percentage removal (85.16%) and metal uptake (21.26 $mg{\cdot}g^{-1}$) can be observed. For BPMC adsorbent reported in the literature that deployed aqueous Pd(II) solutions, with batch adsorption parameters of 2 pH, 300 min contact time and 10 g L^{-1} adsorbent dosage, the removal percentage and capacity are 98% and 16.8 $mg{\cdot}g^{-1}$, respectively [12]. Hence, it has been once again inferred that the adsorption characteristics of ELP solutions are quite distinct from those reported for aqueous solutions.

3.3.3. Effect of dosage

Fig. 5(c) depicts the effect of adsorbent dosage on adsorption capacity and removal efficiency with variation in adsorbent dosage. For an optimal pH and contact time of 12 and 300 min, respectively, the adsorbent removal percentage and capacity can be evaluated to vary from 32.96% to 95.46% and 16.49 to 6.81 $mg{\cdot}g^{-1}$, respectively, for a variation in adsorbent dosage from 1 to 7 $g{\cdot}L^{-1}$. The maximum removal percentage (97.04%) and capacity (8.08 $mg{\cdot}g^{-1}$) exist at an optimal adsorbent dosage of 6 $g{\cdot}L^{-1}$. The literature conveys that for BPMC adsorbent and Pd(II) aqueous solutions, the optimal adsorbent dosage is 10 $g{\cdot}L^{-1}$ at which the capacity and removal percentage have been evaluated as 6.8 $mg{\cdot}g^{-1}$ and 98%, respectively. Hence, it is evident that the optimal dosage reported in the literature (BPMC adsorbent) for aqueous solutions is higher in comparison with that obtained for CH-AC-C. However, removal percentage is higher in the literature than that obtained in this work and capacity is higher for CH-AC-C adsorbent than BPMC [12]. Therefore, it is essential to experimentally investigate the adsorbent for application with ELP solutions and the assumption to consider adsorbent characteristics for aqueous and ELP solutions are similar is erroneous. The lower optimal dosage of the adsorbent (6 $g{\cdot}L^{-1}$) is due to the higher adsorbent surface area (1,317 $m^2{\cdot}g^{-1}$).

3.3.4. Effect of initial Pd(II) solution concentration

Based on preliminary batch adsorption experiments conducted for CH-AC-C adsorbent, the optimum set of adsorption parameters are 12 pH, 300 min contact time and 6 $g{\cdot}L^{-1}$ adsorbent dosage. Corresponding optimal parameters for both CH-AC-I and CH-AC-IS adsorbents have been evaluated as 10, 300 min and 6 $g{\cdot}L^{-1}$, respectively. For CH-AC-C adsorbent, synthetic ELP solutions with and without surfactant were investigated to evaluate the role of initial Pd(II) concentration.

For CH-AC-I and CH-AC-IS adsorbents, synthetic ELP solutions without CTAB surfactant were used for evaluating initial concentrations effect. For all cases, Pd(II) concentration was varied from 50 to 500 mg·L^{-1}. For the cases where CTAB was considered, the concentration of surfactant was 2 CMC.

Figs. 6(a) and (b) present the variation of removal percentage and adsorption capacity for all cases. These correspond to Pd(II) adsorption from synthetic ELP solutions for various cases, namely (a) case without surfactant on CH-AC-I adsorbent, (b) case without surfactant on CH-AC-IS adsorbent, (c) case without surfactant on CH-AC-C adsorbent and (d) case with surfactant on CH-AC-C adsorbent. For comparison, literature data for Pd(II) adsorption from aqueous solutions on BPMC adsorbent have been presented. For a variation in Pd(II) solution concentration from 50 to 500 mg·L^{-1}, highest Pd(II) removal percentage was obtained for case (d) (98.04%–88.87%) followed by case (c) (97.04%–84.17%), case (b) (78.78%–51.41%) and case (a) 68.78%–34.81%. In comparison with literature, only CH-AC-C adsorbent provided better percentage removal than values reported for BPMC. Thus, the prepared adsorbent was effective for Pd(II) adsorption from synthetic ELP solutions, with and without addition of CTAB surfactant.

It can be also analyzed from Fig. 6(b) that adsorption capacity increased almost linearly with an increase in initial feed concentration. A comparison of adsorption capacity for all cases with literature confirms that only CH-AC-C gave higher values of adsorption capacity. The adsorption capacities have been evaluated to be best for case (d) (8.17–74.06 mg·g^{-1}) followed by case (c) (8.08–70.14 mg·g^{-1}), case (b) (6.56–42.54 mg·g^{-1}) and case (a) (5.73–29.01 mg·g^{-1}). Thus, based on adsorption capacity and percentage removal profiles for various adsorbents, it can be inferred that cross-linked chitosan composites perform better than chitosan-impregnated adsorbents. Although literature data do not confirm the efficacy of chitosan-impregnated adsorbents, this work confirmed that impregnation is ineffective to maximize Pd(II) removal percentage and adsorption capacity of composite adsorbents. Thus, cross-linking of chitosan needs to be thoroughly evaluated from preparation as well as process engineering perspectives. The significant variation in Pd(II) characteristics for CH-AC-C adsorbent in comparison with BPMC [12] is possibly due to variation in solution pH (which was 2 in literature and 10–12 for investigated cases) and inclusion of other chemicals such as disodium EDTA, NH_3 and optional CTAB surfactant [12,34].

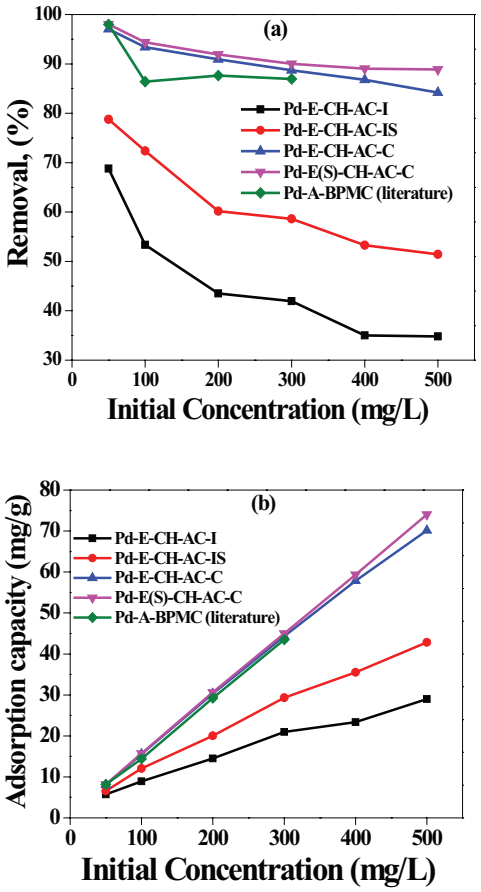

Fig. 6. Effect of initial Pd(II) solution concentration on Pd(II) adsorption characteristics for CH-AC-I, CH-AC-IS, CH-AC-C adsorbents: (a) percentage removal and (b) adsorption capacity.

The prepared synthetic ELP solutions are in basic pH range and in this range, it is well known that chitosan is chemically stable. From available literature, it has been found that chitosan is chemically unstable for a pH less than 6 and greater than 13. During several pH studies conducted for both impregnated and cross-linked adsorbents, no weight loss has been existent for both impregnated and cross-linked adsorbents in the pH range of 2–13. However, as a general precautionary rule, it can be envisaged that the prepared adsorbents are highly promising to serve as adsorbents in the pH range of 6–13 and are not recommended for Pd(II) from acidic media due to the limitation of chitosan. Hence, the suggested methodology to recover Pd(II) from synthetic ELP solutions (in basic pH range) using said cross-linked adsorbent is valid.

3.4. Modelling

3.4.1. Batch equilibrium models

For all cases, Figs. 7(a) and (b), respectively, illustrate fitness plots of batch adsorption data with Langmuir and Freundlich isotherm models. The cases correspond to (a) CH-AC-I using ELP solutions without surfactant, (b) CH-AC-IS using ELP solutions without surfactant, (c) CH-AC-C using ELP solutions without surfactant and (d) CH-AC-C using ELP solutions with 2 CMC CTAB concentration. For these cases, the regression coefficient (R^2) values are 0.915, 0.926, 0.951 and 0.832 (cases (a), (b), (c) and (d)), respectively. Corresponding separation factor (K_R) values are 0.266, 0.001, 0.298 and 0.308 for cases (a)–(d), respectively, and these convey that the adsorbents are favourable for the adsorbent. Other parameters including Langmuir constant are presented in Table 3.

Among all cases, Pd(II) adsorption on CH-AC-C (case (d)) provided best fitness for Langmuir isotherm with an estimated monolayer adsorption capacity of 95.23 mg·g^{-1}. Corresponding experimentally obtained monolayer capacity for CH-AC-C are comparable (70.14 and 74.06 mg·g^{-1}, respectively, for cases without and with CTAB surfactant contained

Pd(II) solution concentration of 50–500 mg·L^{-1}). These values are higher than reported values of adsorption capacity (43.48 mg·g^{-1}) for a solution concentration of 300 mg·L^{-1}. Based on evaluated RMS error values, it can be concluded that significant error exists for fitness of Langmuir isotherm and model fitness is not promising.

For all cases, Fig. 7(b) represents fitness plot for batch adsorption data with Freundlich isotherm model. Regression coefficient (R^2) values correspond to 0.987, 0.994, 0.996 and 0.997 for cases (a)–(d), respectively. Thus, it can be concluded that Freundlich isotherm had good fitness with measured data. Table 4 summarizes Freundlich isotherm parameters obtained for various cases. For various cases, it can be observed that k_f and n varied from 1.23 to 7.29 and 11.17 to 1.15. Thus, it is apparent that heterogeneous phenomena occur for Pd(II) adsorption from ELP solutions without and with CTAB surfactant using CH-AC-C adsorbent. For comparison purposes, it can be noted that for BPMC adsorbent, Sharififard et al. [12] reported the fitness of Freundlich isotherm with parameters such as regression coefficient (R^2), k_f and n specified as 0.99, 8.11 and 2.08, respectively, for Pd(II) solution concentration of 50–300 mg·L^{-1}

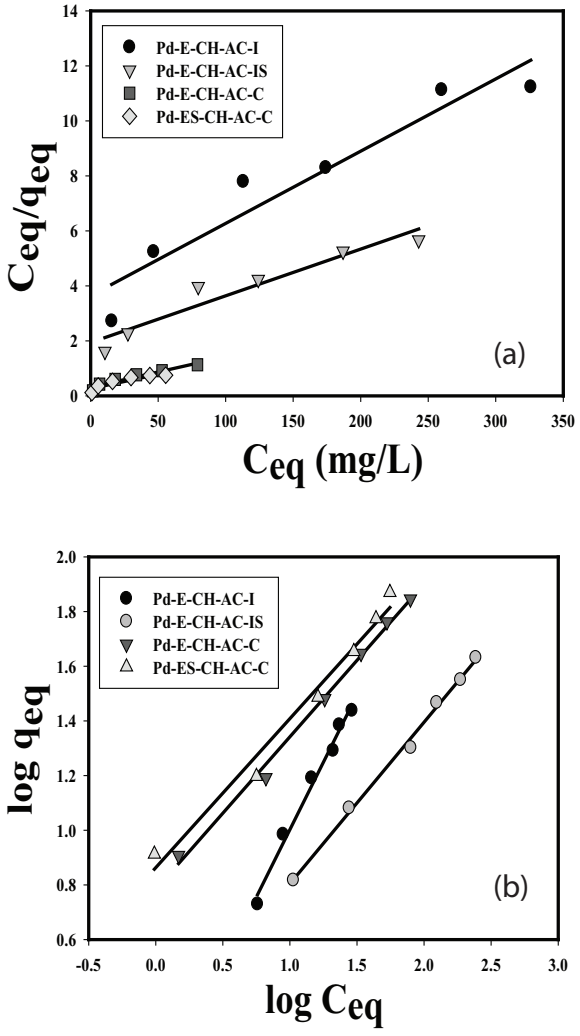

Fig. 7. Fitness of (a) Langmuir and (b) Freundlich isotherm models for Pd-CH-AC-I, Pd-CH-AC-IS and Pd-CH-AC-C cases.

A comparative assessment of Pd(II) adsorption characteristics obtained for CH-AC-I, CH-AC-IS and CH-AC-C adsorbents and literature data are presented in Table 5. Pd(II) adsorption characteristics of commercial activated carbon and laboratory prepared BSAC were comparable for various cases such as agitation and sonication-assisted adsorption. Among all adsorbents, only CH-AC-C provided excellent adsorption characteristics. Deviations in solution formulations need to be noted for comparative purposes, as literature data correspond to aqueous solution-based Pd(II) adsorption, which is not the case in this study. Summarizing the comparison, it can be concluded that the CH-AC-C adsorbent is effective for Pd(II) adsorption and reuse from spent ELP rinse waters [35]. Further experimentation in this regard is necessary. Preliminary desorption studies have been targeted in this study to indicate the efficacy of the adsorbent for Pd reutilization purpose.

3.4.2. Fitness of kinetic models

Among pseudo-first-order and pseudo-second-order kinetic models, the measured kinetic data during Pd(II) adsorption on CH-AC-C using CTAB-containing solutions, pseudo-first-order model did not fit well (not shown). However, good fitness is apparent for second-order kinetic model. Fig. 8 presents the fitness of second-order kinetic model for measured kinetic data for the case of 2 CMC surfactant solution concentration and Pd(II) solutions with variant concentrations of 50–500 mg·L^{-1}. Corresponding model parameters and errors are summarized in Table 6. As presented in Table 6, there is a good agreement with the q_e values determined experimentally and from pseudo-second-order model. Similar modelling trends exist for data obtained with other sets of Pd(II) solution concentrations.

3.5. Desorption studies

Table 7 summarizes the eluent efficiency of CH-AC-C adsorbent. CH-AC-C adsorbent that attained saturated

Table 3
Summary of Langmuir model fitness parameters to represent Pd(II) batch adsorption on CH-AC-I, CH-AC-IS and CH-AC-C adsorbents

Case	R^2	q_{max} (mg·g^{-1})	b	K_R	RMS error
Pd-CH-AC-I	0.915	38.02	0.00723	0.2982	8.78
Pd-CH-AC-IS	0.926	58.82	0.00878	0.0016	6.14
Pd-CH-AC-C	0.951	90.91	0.03486	0.26603	13.95
Pd-CH-AC-C-S	0.832	95.23	0.04024	0.308752	21.68

adsorption state with 300 mg·L^{-1} initial Pd(II) solution concentration was evaluated for its elution efficiency in the conducted batch desorption study. For the case, the experimentally determined capacity corresponds to 44.35 mg·g^{-1}. Based on the Pd(II) solution concentrations obtained after desorption study, it has been evaluated that Pd(II) elution efficiency is significantly lower using 0.1 M HCl. For this case, the equilibrium Pd(II) concentration on the adsorbent after desorption has been estimated to be 43.11 mg·L^{-1}, which is very high and hence not promising. This corresponds to a desorption efficiency of 2.8% for 0.1 M HCl. For NaOH-based desorption study, equilibrium concentration has been estimated to be about 33.84 mg·L^{-1} which is significantly high and conveys a desorption efficiency of 23.67%. On comparing desorption efficiency for the two cases, it can be observed that NaOH gave a higher desorption performance. Hence, the use of a strong base like NaOH is favourable for desorption studies of Pd(II) adsorbed from spent ELP solutions.

The overall desorption efficiency is not significantly high or promising for chitosan–AC adsorbents. Therefore, the applicability of Pd(II)-adsorbed CH-AC-C for desorption is limited and product development by targeting methodologies such as catalysis would be appropriate to serve as application for Pd(II)-adsorbed CH-AC-C adsorbent. Further, lower desorption efficiencies confirm irreversible chemisorption and this is in agreement with the insights gained from FTIR spectral analysis.

Table 4
Summary of Freundlich isotherm fitness parameters to represent Pd(II) batch adsorption on CH-AC-I, CH-AC-IS and CH-AC-C adsorbents

Case	R^2	k_f	n	RMS error
Pd-CH-AC-I	0.987	1.228	11.173	1.108
Pd-CH-AC-IS	0.994	1.634	4.686	0.5562
Pd-CH-AC-C	0.996	6.06	1.278	0.5219
Pd-CH-AC-C-S	0.997	7.29	1.1587	3.8752

4. Conclusions

This work provided several important inferences based on carried out rigorous experimental investigations. First, impregnation process allowed 50%–60% chitosan adsorption to AC porous structure but reduced its surface area, which is not the case for CH-AC-C adsorbent. Second, the best performing CH-AC-C adsorbent provided optimal adsorption characteristics at 12 pH, 300 min contact time and 6 g·L^{-1} adsorbent dosage. Third, the adsorbent provided comparatively better adsorption capacities and Pd(II) removal percentage from synthetic ELP solutions than aqueous solutions [12]. Desorption studies affirmed maximum desorption (23.6%) with 0.1 N NaOH solutions which is not promising for Pd(II) reuse applications. Hence, based on promising adsorption characteristics but not desorption characteristics, the CH-AC-C adsorbent is suggested to be applicable as a catalyst after Pd(II) adsorption for low temperature applications such as hydrogenation in wastewater streams [36], hydrodechlorination of phenols [37] and in situ H_2O_2 generation for phenol dehydration [38,39].

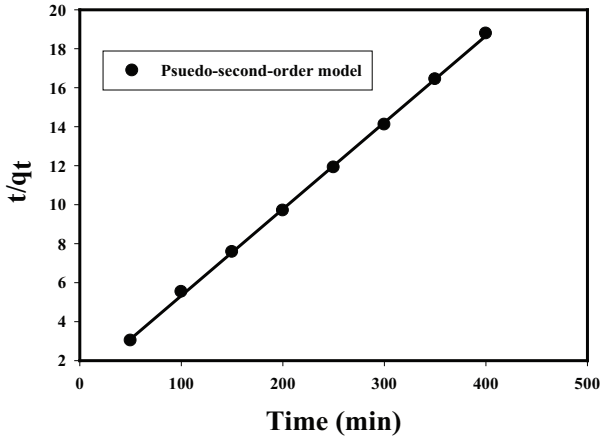

Fig. 8. Fitness of pseudo-second-order kinetic model for CH-AC-C adsorbent with 2 CMC CTAB-containing Pd(II) synthetic ELP solutions.

Table 5
Pd(II) adsorption capacities of various adsorbents

Adsorbent	Type of solution	Pd solution concentration (feed; mg·L^{-1})	Adsorbent capacity (mg·g^{-1})	Reference
CH-AC-I	Synthetic ELP solution	50–500	5.73–29.01	Present work
CH-AC-IS			6.5–42.84	
CH-AC-C			8.08–70.14	
CH-AC-C	ELP solution + CTAB		8.17–74.06	
Activated carbon	Aqueous chloride solution	20–225	1.5–27	[9]
Thiourea-modified chitosan microspheres	Aqueous	10–400	8.28–112.4	[10]
Activated carbon	Pd (A)	50–300	5.3–35.7	[11]
BPMC			6–43.4	
Racomitrium lanuginosum	Aqueous	25–300	5–30.2	[31]

Table 6
Model parameters for pseudo-second-order model to represent Pd(II) adsorption kinetics of CH-AC-C adsorbent and 2 CMC CTAB containing synthetic ELP solutions

C_e (mg·L^{-1})	q_e (mg·g^{-1})		R^2	$k_2 \times 10^{-3}$ (g·mol·min^{-1})	Error			
	Exp	Cal			RMS	Average	Maximum	Minimum
50	21.3	22.5	0.9996	2.21	1.47	1.17	3.62	0.06

Table 7
Batch desorption characteristics of CH-AC-C adsorbent prepared with 300 mg·L^{-1} initial Pd(II) solution concentration

Reagent used	Chemical used	Adsorbent capacity (mg·g^{-1})	Final solution concentration (mg·L^{-1})	Equilibrium adsorbent concentration (mg·g^{-1})	Percentage recovery
HCl	0.1 M	44.345	2.96	43.106	2.792
NaOH	0.1 M	44.345	25.6	33.835	23.698

Acknowledgements

The authors thankfully acknowledge the Department of Chemical Engineering and Central Instrumental Facility, Indian Institute of Technology Guwahati for providing necessary facilities for carrying out this research.

References

[1] J. Kielhorn, C. Melber, D. Keller, I. Mangelsdorf, Palladium – a review of exposure and effects to human health, Int. J. Hyg. Environ. Health, 205 (2002) 417–432.
[2] F.C. Wu, R.L. Tseng, R.S. Juang, Preparation of activated carbons from bamboo and their adsorption abilities for dyes and phenol, J. Environ. Sci. Health, Part A, 34 (1999) 1753–1775.
[3] Y.J. Hsieh, Z. Teng, Industrial Wastewater Treatment Kyoto, Imperial College Press, London, 2000.
[4] K. Mizuta, T. Matsumoto, Y. Hatate, K. Nishihara, T. Nakanishi, Removal of nitrate-nitrogen from drinking water using bamboo powder charcoal, Bioresour. Technol., 95 (2004) 255–257.
[5] J.C. Chaston, E.J. Sercombe, Palladium-on-charcoal catalysts: some effects of variables on hydrogenation activity, Platinum Met. Rev., 5 (1961) 122–125.
[6] A. Ramesh, H. Hasegawa, W. Sugimoto, T. Maki, K. Ueda, Adsorption of gold(III), platinum(IV) and palladium(II) onto glycine modified crosslinked chitosan resin, Bioresour. Technol., 99 (2008) 3801–3809.
[7] D.H.K. Reddy, K. Vijayaraghavan, J.A. Kim, Y. Yun, Valorisation of post-sorption materials: opportunities, strategies, and challenges, Adv. Colloid Interface Sci., 242 (2016) 35–58.
[8] N. Das, Recovery of precious metals through biosorption — a review, Hydrometallurgy, 103 (2010) 180–189.
[9] R.C. Bansal, M. Goyal, Activated Carbon Adsorption, CRC Press, Taylor and Francis Group, 6000 Broken Sound Parkway NW, Suite 300, Boca Raton, FL-33487-2742, 2005.
[10] H. Kasaini, M. Goto, S. Furusaki, Selective separation of Pd(II), Rh(III), and Ru(III) ions from a mixed chloride solution using activated carbon pellets, Sep. Sci. Technol., 35 (2000) 1307–1327.
[11] L. Zhou, J. Liu, Z. Liu, Adsorption of platinum(IV) and palladium(II) from aqueous solution by thiourea-modified chitosan microspheres, J. Hazard. Mater., 172 (2009) 439–446.
[12] H. Sharififard, M. Soleimani, F.Z. Ashtiani, Evaluation of activated carbon and bio-polymer modified activated carbon performance for palladium and platinum removal, J. Taiwan Inst. Chem. Eng., 43 (2012) 696–703.
[13] Y. Rajesh, G. Namrata, U. Ramgopal, Ni(II) adsorption characteristics of commercial activated carbon from synthetic electroless plating solutions, Desal. Wat. Treat., 57 (2016) 13807–13817.
[14] D.H.K. Reddy, S. Lee, Synthesis and characterization of a chitosan ligand for the removal of copper from aqueous media, J. Appl. Polym. Sci., 6 (2013) 4542–4550.
[15] D.H.K. Reddy, S. Lee, Application of magnetic chitosan composites for the removal of toxic metal and dyes from aqueous solutions, Adv. Colloid Interface Sci., 201–202 (2013) 68–93.
[16] D.H.K. Reddy, S. Lee, Three-dimensional porous spinel ferrite as an adsorbent for Pb(II) removal from aqueous solutions, Ind. Eng. Chem. Res., 52 (2013) 15789–15800.
[17] D.H.K. Reddy, Y. Yun, Spinel ferrite magnetic adsorbents: alternative future materials for water purification, Coord. Chem. Rev., 315 (2016) 90–111.
[18] H. Wang, C. Bao, F. Li, X. Kong, J. Xu, Preparation and application of 4-amino-4′-nitro azobenzene modified chitosan as a selective adsorbent for the determination of Au(III) and Pd(II), Microchim. Acta, 168 (2010) 99–105.
[19] S. Woińska, B. Godlewska-Żyłkiewicz, Determination of platinum and palladium in road dust after their separation on immobilized fungus by electrothermal atomic absorption spectrometry, Spectrochim. Acta, Part B, 66 (2011) 522–528.
[20] C. Phalakornkule, J. Foungchuen, T. Pitakchon, Impregnation of chitosan onto activated carbon for high adsorption selectivity towards CO_2: CO_2 capture from biohydrogen, biogas and flue gas, J. Sustain. Energy Environ., 3 (2012) 153–157.
[21] Y. Rajesh, U. Ramagopal, Effect of surfactant and sonication on Pd(II) adsorption from synthetic electroless plating solutions using commercial activated charcoal adsorbent, Desal. Wat. Treat., 57 (2016) 26073–26088.
[22] S. Nagireddi, V. Katiyar, R. Uppaluri, Pd(II) adsorption characteristics of glutaraldehyde cross-linked chitosan copolymer resin, Int. J. Biol. Macromol., 94 (2017) 72–84.
[23] M. Merdivan, R.S. Aygün, N. Külcü, Flame AAS determination of platinum, palladium, and rhodium in catalysts, At. Spectrosc., 18 (1997) 122–126.
[24] Y. Rajesh, M. Pujari, R. Uppaluri, Equilibrium and kinetic studies of Ni (II) adsorption using pineapple and bamboo stem based adsorbents, Sep. Sci. Technol., 49 (2014) 533–544.
[25] Y. Yang, Y. Chun, G. Sheng, M. Huang, pH-dependence of pesticide adsorption by wheat-residue-derived black carbon, Langmuir, 20 (2004) 6736–6741.
[26] I. Langmuir, The adsorption gases on plane surface of glass, mica and platinum, J. Am. Chem. Soc., 40 (1918) 1361–1403.
[27] H.M.F. Freundlich, Over the adsorption in solution, J. Phys. Chem., 57 (1906) 385–470.
[28] V.C. Srivastava, M.M. Swamy, I.D. Mall, B. Prasad, I.M. Mishra, Adsorptive removal of phenol by bagasse fly ash and activated carbon: equilibrium, kinetics and thermodynamics, Colloids Surf., A, 272 (2006) 89–104.
[29] C. Aharoni, M. Ungarish, Kinetics of activated chemisorption. Part 2.—Theoretical models, J. Chem. Soc. Faraday Trans. 1, 73 (1977) 456–464.
[30] Y.S. Ho, G. McKay, Pseudo-second order model for sorption processes, Process Biochem., 34 (1999) 451–465.

[31] K.S.W. Sing, D.H. Everett, R.A.W. Haul, L. Moscou, R.A. Pierotti, J. Rouquerol, T. Siemieniewska, Reporting physisorption data for gas/solid systems with special reference to the determination of surface area and porosity, Pure Appl. Chem., 57 (1985) 603–619.
[32] L.D. Gelb, K.E. Gubbins, Pore size distributions in porous glasses: a computer simulation study, Langmuir, 15 (1999) 305–308.
[33] S.A. Dastgheib, D.A. Rockstraw, A model for the adsorption of single metal ion solutes in aqueous solution onto activated carbon produced from pecan shells, Carbon, 40 (2002) 1843–1851.
[34] C.A. Snyders, C.N. Mpinga, S.M. Bradshaw, G. Akdogan, J.J. Eksteen, The application of activated carbon for the adsorption and elution of platinum group metals from dilute cyanide leach solutions, J. S. Afr. Inst. Min. Metall., 113 (2013) 381–388.
[35] S. Paria, K.C. Khilar, A review on experimental studies of surfactant adsorption at the hydrophilic solid–water interface, Adv. Colloid Interface Sci., 110 (2004) 75–95.
[36] E. Díaz, A.F. Mohedano, L. Calvo, M.A. Gilarranz, J.A. Casas, J.J. Rodríguez, Hydrogenation of phenol in aqueous phase with palladium on activated carbon catalysts, Chem. Eng. J., 131 (2007) 65–71.
[37] L. Calvo, A.F. Mohedano, J.A. Casas, M.A. Gilarranz, J.J. Rodríguez, Treatment of chlorophenols-bearing wastewaters through hydrodechlorination using Pd/activated carbon catalysts, Carbon, 42 (2004) 1377–1381.
[38] A. Saria, D. Mendil, M. Tuzen, M. Soylak, Biosorption of palladium(II) from aqueous solution by moss (*Racomitrium lanuginosum*) biomass: equilibrium, kinetic and thermodynamic studies, J. Hazard. Mater., 162 (2009) 874–879.
[39] M.S. Yalfani, New Catalytic Advanced Oxidation Processes for Wastewater Treatment, Department of Chemical Engineering, Universitat Rovira i Virgili, Tarragona, 2011.